SAGA-HE-208-04 (hep-ph/0408135) July 31, 2004

Nuclear corrections of parton distribution functions

M. Hirai [(a)], S. Kumano [(b),*], and T.-H. Nagai [(b)]

(a) Institute of Particle and Nuclear Studies, KEK
1-1, Ooho, Tsukuba, Ibaraki, 305-0801, Japan

(b) Department of Physics, Saga University
Saga, 840-8502, Japan

Talk at the Third International Workshop on
Neutrino-Nucleus Interactions in the Few GeV Region (NuInt04)

Gran Sasso, Italy, March 17 - 21, 2004

(talk on March 17)

* URL: http://hs.phys.saga-u.ac.jp.

to be published in Nucl. Phys. B Supplements

Nuclear corrections of parton distribution functions

M. Hirai [a] *, S. Kumano [b] †, and T.-H. Nagai [b] ‡

[a]Institute of Particle and Nuclear Studies, KEK, 1-1, Ooho, Tsukuba, Ibaraki, 305-0801, Japan

[b]Department of Physics, Saga University, Saga, 840-8502, Japan

We report global analysis results of experimental data for nuclear structure-function ratios $F_2^A/F_2^{A'}$ and proton-nucleus Drell-Yan cross-section ratios $\sigma_{DY}^{pA}/\sigma_{DY}^{pA'}$ in order to determine optimum parton distribution functions (PDFs) in nuclei. An important point of this analysis is to show uncertainties of the distributions by the Hessian method. The results indicate that the uncertainties are large for gluon distributions in the whole x region and for antiquark distributions at $x > 0.2$. We provide a code for calculating any nuclear PDFs at given x and Q^2 for general users. They can be used for calculating high-energy nuclear reactions including neutrino-nucleus interactions, which are discussed at this workshop.

1. Introduction

Although parton distribution functions (PDFs) in the nucleon are now determined relatively well in the wide range of x, their nuclear modifications are not determined accurately. There are experimental measurements about nuclear effects on the PDFs, for example nuclear F_2 data, so that their gross properties are known. However, the details are not still determined because available experimental data exist for a limited number of high-energy nuclear reactions.

On the other hand, accurate nuclear parton distribution functions (NPDFs) [1–4] are needed for describing any high-energy nuclear reactions such as heavy-ion and neutrino reactions. The major purpose of this workshop is to discuss nuclear effects on neutrino reactions [5]. Since neutrino-oscillation experiments [6] become more and more accurate, it is now important to take nuclear medium effects into account.

Current oscillation experiments are done in a medium-energy region, so that there are various nuclear effects which contribute to the neutrino reactions. Among them, we investigate nuclear medium effects on the PDFs. Of course, the parton distributions are supposed to be used in the deep inelastic (DIS) region, so that an extension to a smaller Q^2 region becomes important in order to use them for the present neutrino reactions.

In this paper, we report our recent studies on the NPDFs by analyzing the nuclear data on the structure-function ratios $F_2^A/F_2^{A'}$ and Drell-Yan cross-section ratios $\sigma_{DY}^{pA}/\sigma_{DY}^{pA'}$ [2]. We had already reported the NPDF studies on the first version [1] at the NuInt01 workshop [7] and preliminary studies after the first version at the NuInt02 [8].

The most important point in Ref. [2] is that uncertainties of the NPDFs are estimated by the Hessian method. For calculating any nuclear reactions, it is especially important to show the uncertainties which come from the PDFs. Furthermore, Drell-Yan and HERMES data are added into the data set and the charm-quark distributions are included in the new analysis.

This paper consists of the following. In section 2, a method is explained for analyzing F_2 and Drell-Yan data in order to obtain the optimum NPDFs. Analysis results are shown in section 3. We provide a code for calculating the NPDFs at given x and Q^2, and it is explained in section 4. The results are summarized in section 5.

*mhirai@rarfaxp.riken.go.jp
†kumanos@cc.saga-u.ac.jp, http://hs.phys.saga-u.ac.jp
‡03sm27@edu.cc.saga-u.ac.jp

2. Analysis method

The parton distribution functions are expressed in general by two variables, x and Q^2. In lepton-nucleus scattering, the Q^2 is defined by the momentum transfer q: $Q^2 = -q^2$, and the Bjorken scaling variable x is given by $x = Q^2/(2M\nu)$ with the nucleon mass M and the energy transfer ν. The NPDFs are provided by an analytical form at a fixed Q^2 point (Q_0^2). Practically, a NPDF could be expressed by the corresponding nucleonic distribution multiplied by a function w_i:

$$f_i^A(x, Q_0^2) = w_i(x, A, Z)\, f_i(x, Q_0^2). \quad (1)$$

We call w_i a weight function, which indicates nuclear modification. The function is expressed by a number of parameters:

$$w_i(x, A, Z) = 1 + \left(1 - \frac{1}{A^{1/3}}\right) \times \frac{a_i(A, Z) + b_i x + c_i x^2 + d_i x^3}{(1-x)^{\beta_i}}. \quad (2)$$

The parameters are determined by a χ^2 analysis with experimental data on structure functions F_2^A and Drell-Yan cross sections σ_{DY}^{pA}. Because of baryon-number, charge, and momentum conservations, three parameters can be fixed. The cubic functional form of the numerator is motivated by the x dependence of typical data for F_2^A/F_2^D, and the factor $1/(1-x)^{\beta_i}$ is to reproduce the Fermi-motion part at large x. The nuclear dependence $1 - 1/A^{1/3}$ is introduced in Ref. [9] simply by considering nuclear volume and surface contributions to cross sections. Because different physics mechanisms contribute in each x region, the overall $1/A^{1/3}$ dependence would be too simple to describe the nuclear modifications. For the NPDFs f_i^A, we take u_v^A, d_v^A, $\bar{q}^A$, and g^A by assuming flavor symmetric antiquark distributions although they are not symmetric in the nucleon [10].

The parameters are determined by a χ^2 analysis with experimental values. The χ^2 is given by

$$\chi^2 = \sum_j \frac{(R_j^{data} - R_j^{theo})^2}{(\sigma_j^{data})^2}, \quad (3)$$

where σ_j^{data} is an experimental error, and R_j indicates a ratio, $F_2^A/F_2^{A'}$ or $\sigma_{DY}^{pA}/\sigma_{DY}^{pA'}$. Leading-order expressions are used in the theoretical calculations.

The actual calculation is done by running the subroutine `MINUIT`. The subroutine also produces a Hessian matrix H which has information on parameter errors. Using the matrix, we can calculate the uncertainty of a NPDF:

$$[\delta f^A(x)]^2 = \Delta\chi^2 \sum_{i,j} \left(\frac{\partial f^A(x,\xi)}{\partial \xi_i}\right)_{\xi=\hat{\xi}} \times H_{ij}^{-1} \left(\frac{\partial f^A(x,\xi)}{\partial \xi_j}\right)_{\xi=\hat{\xi}}, \quad (4)$$

where ξ_i is a parameter, $\hat{\xi}$ indicates the optimum set of the parameters, and $\delta f^A(x)$ is the uncertainty of the nuclear PDF $f^A(x)$. The $\Delta\chi^2$ value determines a confidence region and it depends on the number of parameters.

The kinematical region of the experimental data for F_2^A and σ_{DY}^{pA} is shown in Fig. 1. In comparison with the nucleon data, the x range is still limited. Namely, the small-x ($x = 10^{-5} - 10^{-3}$) data are not taken. The Drell-Yan data are taken in the large Q^2 region. There are 606 data points for the F_2^A/F_2^D type, 293 for $F_2^A/F_2^{A'}$ ($A' \neq D$), and 52 for the Drell-Yan. The total number of data is 951. These data are taken for the targets: deuteron (D), helium-4 (^{4}He), lithium (Li), beryllium (Be), carbon (C), nitrogen (N), aluminum (Al), calcium (Ca), iron (Fe), copper (Cu), krypton (Kr), silver (Ag), tin (Sn), xenon (Xe), tungsten (W), gold (Au), and lead (Pb).

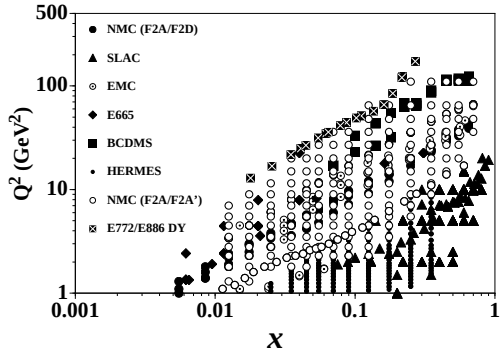

Figure 1. Kinematical region is shown for experimental data.

3. Results

3.1. Comparison with experimental data

The NPDFs in Eqs. (1) and (2) are given at Q_0^2=1 GeV^2, and they are evolved to the experimental Q^2 points for calculating the total χ^2 in Eq. (3). The optimum parameters are obtained by minimizing χ^2. The minimum χ^2 becomes 1489.8 for the 951 data. The uncertainties of the NPDFs are estimated with $\Delta\chi^2$=10.427 in order to show the one-σ-error range. It is chosen by considering that the number of the parameters is nine [2,11].

Each χ^2 contribution is listed in Table 1. There is a tendency that the χ^2 values are large for small nuclei. The Li/D, Be/D, and C/D ratios have χ^2 values, 88.7, 44.1, and 130.8, for the number of data points, 17, 17, and 43 points, respectively.

Table 1
Each χ^2 contribution.

nucleus	# of data	χ^2
^{4}He/D	35	56.0
Li/D	17	88.7
Be/D	17	44.1
C/D	43	130.8
N/D	162	136.9
Al/D	35	43.1
Ca/D	33	42.0
Fe/D	57	95.7
Cu/D	19	11.8
Kr/D	144	126.9
Ag/D	7	12.8
Sn/D	8	14.6
Xe/D	5	2.0
Au/D	19	61.6
Pb/D	5	5.6
F_2^A/F_2^D total	606	872.8
Be/C	15	16.1
Al/C	15	6.1
Ca/C	39	36.5
Fe/C	15	10.3
Sn/C	146	257.3
Pb/C	15	25.3
C/Li	24	78.1
Ca/Li	24	107.7
$F_2^{A_1}/F_2^{A_2}$ total	293	537.4
C/D	9	9.8
Ca/D	9	7.2
Fe/D	9	8.1
W/D	9	18.3
Fe/Be	8	6.5
W/Be	8	29.6
Drell-Yan total	52	79.6
total	951	1489.8

Medium and large size nuclei are generally well reproduced except for the Sn/C and Ca/Li ratios. The Drell-Yan data are also well explained except for the W/Be ratios.

Typical results are shown in Figs. 2 and 3. In Fig. 2, the F_2^{Ca}/F_2^D data are compared with the fit result at Q^2=5 GeV^2. The shaded area is the uncertainty range due to the NPDF uncertainties at Q^2=5 GeV^2. One should note that the experimental data are taken at various Q^2 points which are not equal to 5 GeV^2. Therefore, the curve cannot be, strictly speaking, compared with the data. However, considering that the Q^2 dependence is small in general, we find that the data are reproduced well by the parametrization.

The Drell-Yan data $\sigma_{DY}^{pCa}/\sigma_{DY}^{pD}$ are compared with the fit result in Fig. 3. The parametrization curve and the uncertainty range are calculated at Q^2=50 GeV^2, whereas the data are taken at various Q^2 points. In the region $x < 0.1$, the cross-section ratio is almost the same as the antiquark ratio $\bar{q}^{Ca}/\bar{q}^D$, so that the data play a role of fixing the nuclear antiquark distributions at $x \sim 0.1$.

The actual comparison with the experimental data should be done at the same Q^2 points. In order to estimate the fit result, we show the ratios $(R^{exp} - R^{theo})/R^{theo}$ in Fig. 4. Here, R^{exp} indicates an experimental F_2 ratio and R^{theo} does a

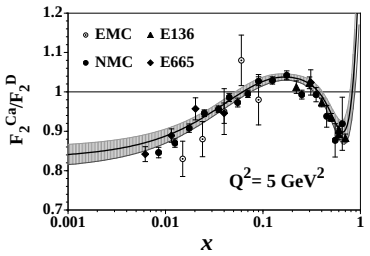

Figure 2. Comparison with the F_2^{Ca}/F_2^D data.

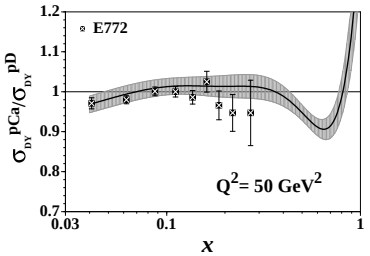

Figure 3. Comparison with the $\sigma_{DY}^{pCa}/\sigma_{DY}^{pD}$ data.

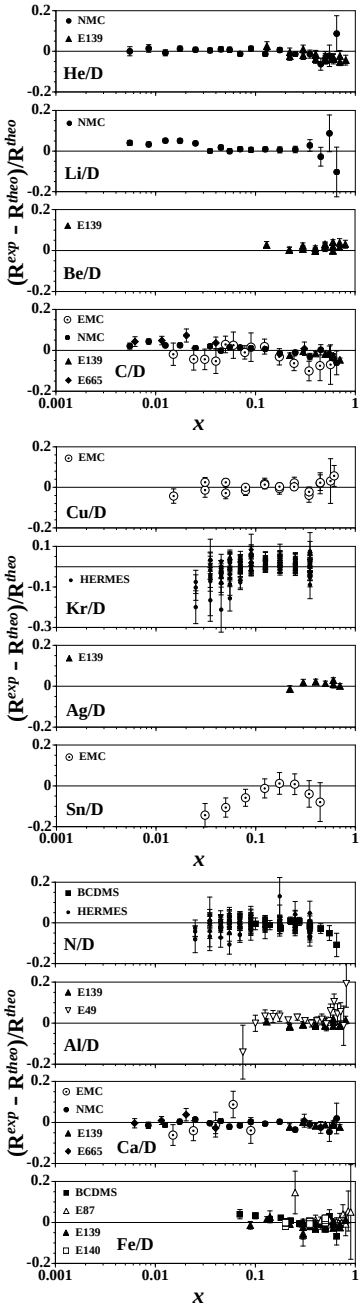

Figure 4. Fit results are compared with experimental data for $R = F_2^A/F_2^D$ at the same experimental Q^2 points. The fractional differences $(R^{exp} - R^{theo})/R^{theo}$ are shown.

ratio by the parametrization. The theoretical ratios are calculated at the experimental Q^2 points. Among the used data, only F_2^A/F_2^D type data are shown in Fig. 4. In general, the data are well explained by the parametrization. However, there are slight deviations in small nuclei as indicated in Table 1. For example, the lithium data at small x are underestimated. On the other hand, the tin data are overestimated at small x. We need more complicated A dependence for explaining all the nuclei.

3.2. Q^2 dependence

Next, Q^2 dependence of F_2 is calculated and it is shown with the F_2^N/F_2^D data in Fig. 5, where N indicates nitrogen. The figure shows that the Q^2 dependence of the ratio F_2^N/F_2^D is not very obvious experimentally, which makes the determination of the nuclear gluon distributions difficult. The ratio tends to decrease with increasing Q^2 at $x = 0.035$ and $x = 0.045$. There is a same tendency in the F_2^{Kr}/F_2^D data by the HERMES collaboration. However, the ratio F_2^{Sn}/F_2^C increases with increasing Q^2 at $x = 0.0125 \sim 0.045$ according to the NMC collaboration [2]. It seems that the Q^2 variations are not consistent each other between the HERMES and NMC data. Since such Q^2 dependence is crucial in determining nuclear gluon distributions, we hope that the Q^2 dependence will be accurately measured in the small-x region.

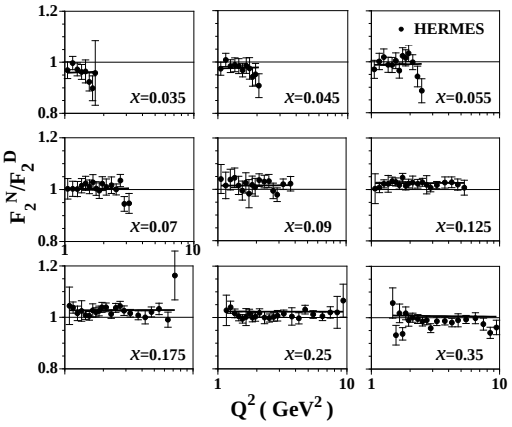

Figure 5. Q^2 dependence of F_2^N/F_2^D is shown in comparison with the data. The curves indicate fit results.

3.3. NPDFs with uncertainties

From the χ^2 fit, we obtain the optimum NPDFs with the uncertainties. As an example, the weight functions are shown for the calcium nucleus in Fig. 6. These functions indicate nuclear modifications of the valence-quark, antiquark, and gluon distributions in the calcium at Q^2=1 GeV^2 by definition. The shaded areas indicate the uncertainties estimated by the Hessian method.

The valence-quark distributions are well determined at medium x by the F_2^A data because the F_2^A is dominated by them in this x region. In the small-x region, the valence distributions are fixed by baryon-number and charge conservations. These are the reasons why the uncertainties are rather small. However, it is worth while investigating the valence-quark shadowing at the NuMI and neutrino-factory projects [12] despite the present result.

The antiquark distributions are determined at small x because of the shadowing data of F_2^A at small x. They are also fixed at $x \sim 0.1$ by the Drell-Yan data. We notice that the uncertainties are fairly small in these regions. However, they cannot be determined at $x > 0.2$ as indicated by the large uncertainties in Fig. 6. We need new experiments such as J-PARC and Fermilab-P906 in this large-x region [13].

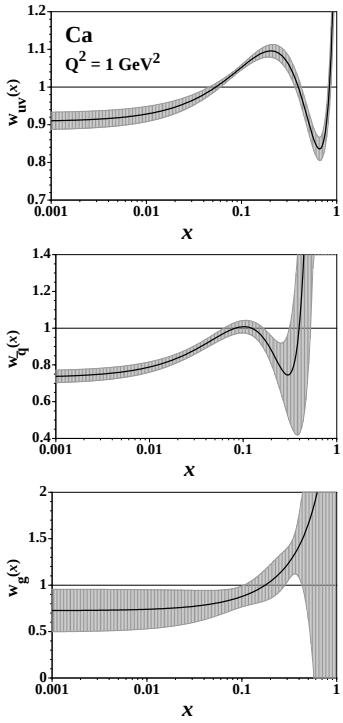

Figure 6. Nuclear modifications of valence-quark, antiquark, and gluon distributions in the calcium nucleus at Q^2=1 GeV^2.

The gluon distributions cannot be fixed at this stage although they seem to be shadowed at small x. In fact, the uncertainties are huge in the whole x region. The difficulty is mainly because accurate scaling violation data are not available at small x as shown in Fig. 5. The Q^2 variations in the $x \sim 0.01$ region are not measured accurately, and it is also obvious from Fig. 1 that the small-x ($x = 10^{-3} \sim 10^{-4}$) data themselves do not exist. In addition, a next-to-leading-order analysis could be important for incorporating the gluon contributions into the parametrization.

From the analysis, we obtain the NPDFs from the deuteron to a heavy nucleus with $A \sim 208$. We provide the NPDFs for general users by providing a code, which is explained in the next section. The NPDFs could be used for any high-energy nuclear reactions. In order to use them for the present neutrino oscillation experiments in a medium-energy region, an extension from the DIS region to the resonance one should be investigated. Such an effort has been done, for example, in Ref. [14] for the structure function F_2 of the nucleon. Obviously, we need a similar study for extending the NPDFs to the smaller Q^2 region in order to calculate nuclear corrections to the cross sections in the neutrino oscillation experiments.

4. Code for calculating NPDFs

A useful code could be obtained from the web site in Ref. [2]. In the package (npdf04.tar.gz), grid data, npdf04 subroutine (npdf04.f), and a sample file (sample.f) are provided. Running the subroutine, one obtains the NPDFs at given x and Q^2 for the analyzed nuclei, D, ^{4}He, Li, Be, C, N, Al, Ca, Fe, Cu, Kr, Ag, Sn, Xe, W, Au, and Pb. The kinematical ranges for the provided NPDFs are $10^{-9} \leq x \leq 1$ and 1 GeV^2 $\leq Q^2 \leq$ 10^8 GeV^2. The smallest x point of the data is x_{min}=0.0055, so that one should note that the

NPDFs at $x < x_{min}$ are not tested experimentally. However, we provide the small-x distributions in case that one uses the NPDFs for integrating them over a wide range of x. The maximum Q^2 of the data is 173 GeV^2. The Q^2 variations above this point are also not tested experimentally. We simply assumed the standard DGLAP Q^2 evolution equations for extending the Q^2 region up to $Q^2 = 10^8$ GeV^2 for feasibility studies of future experimental facilities.

For a nucleus other than the provided ones (D, He, $\cdots$, Pb), the NPDFs could be calculated by following the procedure in Appendix of Ref. [2]. Namely, the nuclear dependent parameters a_{u_v}, a_{d_v}, a_g are calculated by Eq. (A1) of Ref. [2], and other parameter values are taken from Table II. Next, the NPDFs for a nucleus can be calculated at Q^2=1 GeV^2 by using the analytical expressions with the determined parameters. Then, one may evolve the NPDFs to a given Q^2 point by one's Q^2 evolution code or, if it is not available, by the code in Ref. [15]. The analyzed nuclei are up to $A = 208$. However, variations from the lead NPDFs to those of the nuclear matter ($A \to \infty$) are small, so that one may use the analysis results for large nuclei with $A > 208$.

5. Summary

We have investigated a parametrization of NPDFs by analyzing experimental data on F_2^A and Drell-Yan processes. In addition to obtaining the optimum NPDFs, we calculated their uncertainties by the Hessian method. The antiquark distributions at small x and valence-quark distributions are well determined by the data. However, the antiquark distributions at $x > 0.2$ and the gluon distributions cannot be determined reliably. We obviously need future experimental efforts for determining these distributions. One could use the obtained NPDFs by running the provided code.

Acknowledgments

S.K. thanks Profs. F. Cavanna and M. Sakuda for taking care of his participation in this workshop. He was supported by the Grant-in-Aid for Scientific Research from the Japanese Ministry of Education, Culture, Sports, Science, and Technology.

REFERENCES

1. M. Hirai, S. Kumano, and M. Miyama, Phys. Rev. D64 (2001) 034003.
2. M. Hirai, S. Kumano, and T.-H. Nagai, hep-ph/0404093 (Phys. Rev. C in press). The NPDF code could be obtained from http://hs.phys.saga-u.ac.jp/nuclp.html.
3. There are other NPDF studies, for example, K. J. Eskola, V. J. Kolhinen, and P. V. Ruuskanen, Nucl. Phys. B535 (1998) 351; K. J. Eskola, V. J. Kolhinen, and C. A. Salgado, Eur. Phys. J. C9 (1999) 61; D. de Florian and R. Sassot, Phys.Rev. D69 (2004) 074028. See also L. Frankfurt, V. Guzey, and M. Strikman, hep-ph/0303022.
4. There are related talks on the NPDFs at this workshop. See S. Kulagin, B. Kopeliovich, contributions to this workshop.
5. http://nuint04.lngs.infn.it/.
6. M. Sakuda, Nucl. Phys. B112 (2002) 109; E. A. Paschos and J. Y. Yu, Phys. Rev. D65 (2002) 033002.
7. http://neutrino.kek.jp/nuint01/.
8. http://nuint.ps.uci.edu/.
9. I.Sick and D.Day, Phys. Lett. B274 (1992) 16.
10. S. Kumano, Phys. Rep. 303 (1998) 183; G. T. Garvey and J.-C. Peng, Prog. Part. Nucl. Phys. 47 (2001) 203.
11. M. Hirai, S. Kumano, and N. Saito (AAC), Phys. Rev. D69 (2004) 054021.
12. J. G. Morfin, J. Phys. G29 (2003) 1935.
13. J. C. Peng, in KEK proceedings 2000-19, Workshop on Di-lepton Experiments at the 50-GeV PS, edited by J. Chiba and S. Sawada (2000); The P906 Collaboration, proposal for Drell-Yan measurements at the FNAL Main Injector (1999).
14. A. Bodek and U. K. Yang, Nucl. Phys. B112 (2002) 70.
15. M. Miyama and S. Kumano, Comput. Phys. Commun. 94 (1996) 185.